

IBA techniques: Examples of useful combinations for the characterisation of cultural heritage materials

L. Beck^{a,b,*}, L. Pichon^a, B. Moignard^a, T. Guillou^a, P. Walter^a

^a Centre de Recherche et de Restauration des Musées de France (C2RMF), CNRS-UMR 171, Palais du Louvre, 14 quai François Mitterrand, 75001 Paris, France

^b INSTN, CEA Saclay, 91120 Gif sur Yvette, France

ARTICLE INFO

Article history:

Available online 22 April 2011

Keywords:

Ion beam analysis
Cultural heritage
RBS
PIXE
PIGE
Silver
Bone
Coins

ABSTRACT

For many years, ion beam analysis techniques have successfully been used to the study of cultural heritage objects. The chemical composition of work art is usually determined by PIXE, but in many cases, RBS and/or PIGE can provide useful complementary information. RBS gives information about the depth distribution and concentration in light elements, such as carbon and oxygen. In the past years, the experimental facilities at the AGLAE (Accélérateur Grand Louvre d'Analyse Élémentaire) accelerator has been progressively developed in order to apply simultaneously PIXE, PIGE and RBS under optimal conditions using an external beam. This combination is now routinely used for point analyses or mappings. In this contribution, we present several examples of applications: manufacturing technology of lustre-decorated ceramics and silver plating, control of altered or restored surfaces, and quantification of organic phase in painting and bone. The final conclusion is that the association of PIXE with RBS is very attractive for the investigation of cultural heritage objects, in particular of materials containing both mineral and organic components or possessing a multilayered structure. The first results of the production of monochromatic X-rays for radiography purposes by PIXE are also presented.

© 2011 Elsevier B.V. All rights reserved.

1. Introduction

It is now well known that ion beam analysis is a valuable investigation technique for the analysis of objects of the cultural heritage [1]. PIXE has been successfully applied to the determination of the origin of gems [2], obsidian [3] or prehistoric pigments [4] as well as to the analysis of paintings [5] and metals [6–8].

However, PIXE has some limitations, namely the lack of depth information or the low sensitivity to light elements. For these reasons, the external beam of AGLAE (Accélérateur Grand Louvre d'Analyse Élémentaire) has been continuously modified to enable the use of RBS at atmospheric pressure [9]. The facility has more recently been improved in order to perform PIXE and RBS simultaneously [10]. Through this combination, the number of detected elements is increased and depth distribution information provided. This combination, which gave already original results on patination [11] or on Renaissance paintings [12,13], is now routinely used and applied systematically whatever the nature and the structure of the object under investigation.

In the first part of this contribution, different cases, where PIXE and RBS are particularly complementary, will be presented. In the

case of layer-structured materials (e.g. intentional coating of metals, such as gilding and silvering), the analysis can provide technological information about the manufacture of the objects, while for altered surfaces, the PIXE–RBS combination is essential for an accurate quantification of the elements. In addition, the implementation of RBS with PIXE provides data for light element quantification. It will be also shown how the information on light elements and particularly on carbon and oxygen, which are present in organic compounds such as varnish, binder, protective product and in biomaterials such as bone, is useful.

In a second part, preliminary results on X-radiography performed using monoenergetic X-rays produced by proton bombardment of a metal target, will be discussed.

2. The PIXE–RBS combination

2.1. The experimental setup

In the past years, two different approaches were developed for the nozzle design of the AGLAE external beam line [10].

A first setup was based on separated and mechanically independent components: a beam extraction nozzle with a 100 nm thick Si₃N₄ window, two Si(Li) X-ray detectors, one surface barrier (SB) detector mounted in a small chamber under vacuum separated by a 100 nm thick Si₃N₄ window, one HP-Ge detector and a dose

* Corresponding author. Present address: CEA, DEN, Service de Recherches de Métallurgie Physique, JANNuS Laboratory, 91120 Gif sur Yvette, France.

E-mail address: lucile.beck@cea.fr (L. Beck).

detector using a PIN diode Peltier cooled detector for measuring the Si X-rays emitted by the exit window.

A second, more elegant, setup was then developed by integrating the SB detector in the exit nozzle in order to reduce the size of the previous set-up and improve the beam monitoring. The integrated annular SB detector, placed at of 170° , was used for both the RBS measurement and the dose monitoring. This compact system was mainly utilised for the simultaneous PIXE and RBS using 6 MeV $^4\text{He}^{2+}$ -ions [14].

Presently, an upgraded version of the first arrangement is mainly used (Fig. 1). Three main modifications have been introduced:

- (1) The vacuum inside the nozzle has been improved by adding a small turbo-pump on the back of the beam extractor. A better vacuum reduces the carbon deposition on the Si_3N_4 membrane and the quality (shape and size) of the beam is improved.
- (2) The RBS detector is mechanically interdependent of the nozzle allowing more accurate and easier adjustments preserving the alignments. The RBS detector is now permanently mounted for all the experiments.
- (3) The dose monitoring is still based on the principle of the detection of the Si K-line emitted by the Si_3N_4 exit window but the design was improved by using a weightless system. This system consists of an X123-SDD detector (area: 7 mm^2 , crystal thickness: $450\text{ }\mu\text{m}$, Be window thickness: $25\text{ }\mu\text{m}$), a preamplifier, a digital processor, and a power supply. The installed version has the detector and the preamplifier

removed from the electronics box and connected with a 9-in. flexible cable. The detector is mounted in air, in a housing mechanically connected to the beamline. The tightness between the vacuum of the beamline and the atmospheric pressure is guaranteed by a $125\text{ }\mu\text{m}$ Be membrane. The SDD detector covers a wide range of counting rate and so, the dose measurement is reliable independent of the particle flux.

This recent configuration, now routinely used, gives access to complementary information by the simultaneous detection of X-rays, gamma-rays and backscattered particles. The same arrangement is also utilised for elemental mappings [15].

2.2. Examples

2.2.1. Intentional surface modification: metal decoration

Noble metal layers have often been used in the past to decorate objects made of materials of lesser value (base metal, ceramics, glass, wood, plaster, etc.). The most widespread technique used metal foils but, in the particular case of lustre-decorated ceramics, the metal is in nanoparticles form included in the glaze. The iridescent and metallic appearance of lustre-decorated ceramics originates in this thin layer of silver or copper nanoparticles.

During the past 10 years, considerable efforts have been made to investigate the chemical and physical structures and the optical properties of lustre-decorated ceramics. IBA has been applied to examine the fabrication technology. For instance, studies have been carried out on Middle-East, Spanish and Italian productions [16–18]. The combination of PIXE and RBS has highlighted the differences or similarities among the various productions. The evolution of the lustre-decorated ceramic technology has been elucidated by detailed observation of the composition and the thickness of the copper and/or silver nano-particles film as well as of the composition of the glaze layer and that of the ceramic body. The typical metallic layers are between 50 and 300 nm thick with various concentrations of copper and silver depending on the colour and the production workshop. The metallic layer can directly be found on the surface of ceramics such as, for example, Hispano-Moresque lustres dated before the beginning of the 16th century, but a glaze layer of 100 nm above the metallic nanoparticles can be observed for earlier Islamic and the Italian majolica productions. All these data were obtained by performing two successive experiments, using 3 MeV H^+ for the terra cotta characterisation and 3 MeV He^{2+} for the glaze and metal layers study. A detailed summary report on the IBA contribution to the knowledge of the lustre-decorated ceramics is in progress.

Another useful application field of IBA is the study of the plating manufacturing processes. Gilding has extensively been studied [19] but the silvering processes are less known. The discovery of a large hoard of coins of the 16th century [20] containing several counterfeit coins offered an opportunity to examine their manufacturing technology and more specifically, to investigate the formation of the silver plating layer on their surface. A 3 MeV proton beam was used for RBS and PIXE. RBS was applied to the determination of the plating layer thickness while PIXE was found to be necessary for the determination of the elemental composition of the layer and that of the copper substrate. Two main types of silvering methods were brought to light. Silvering containing mercury was observed for 14 counterfeit coins among which 11 were imitations of the coat of arms of Johann August von der Pfalz-Veldenz (1598–1611, Count palatine of Veldenz-Lützelstein, Upper Rhine circle, Holy Roman Empire). The thickness of the layer was between 1 and $2\text{ }\mu\text{m}$ and the composition 50–60 wt.% Hg, and 50–40 wt.% Ag depending on the coin (Fig. 2). This composition

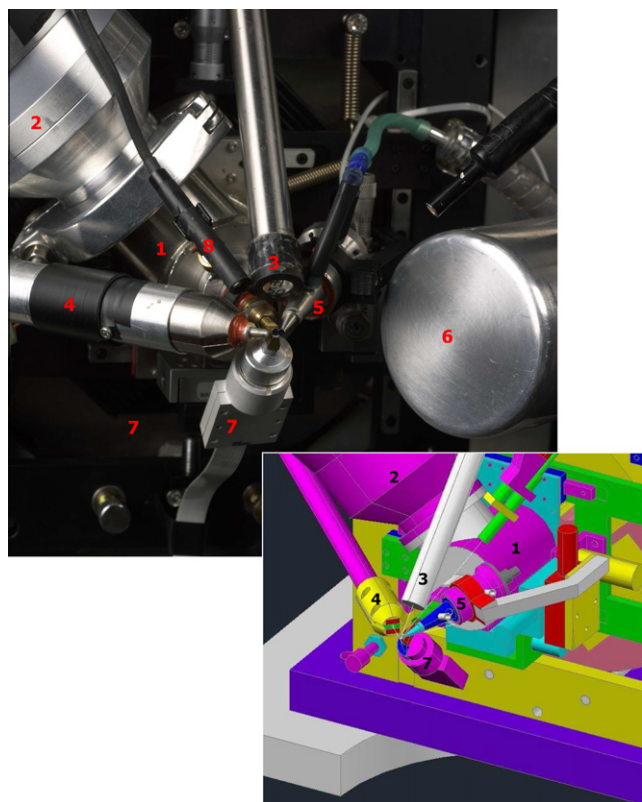


Fig. 1. External beam set-up used for simultaneous PIXE-RBS-PIGE. (1) Beam extraction nozzle with a Si_3N_4 window; (2) turbo-pump; (3) high energy Si(Li) X-ray detector equipped with a $6\text{-}\mu\text{m}$ Be window, solid angle 100 mSr ; (4) low energy Si(Li) X-ray detector equipped with a deflection magnet, $0.25\text{-}\mu\text{m}$ BN window, He flux, solid angle 10 msr ; (5) RBS detector; (6) gamma detector; (7) dose detector: SDD Peltier cooled detector; (8) camera for positioning.

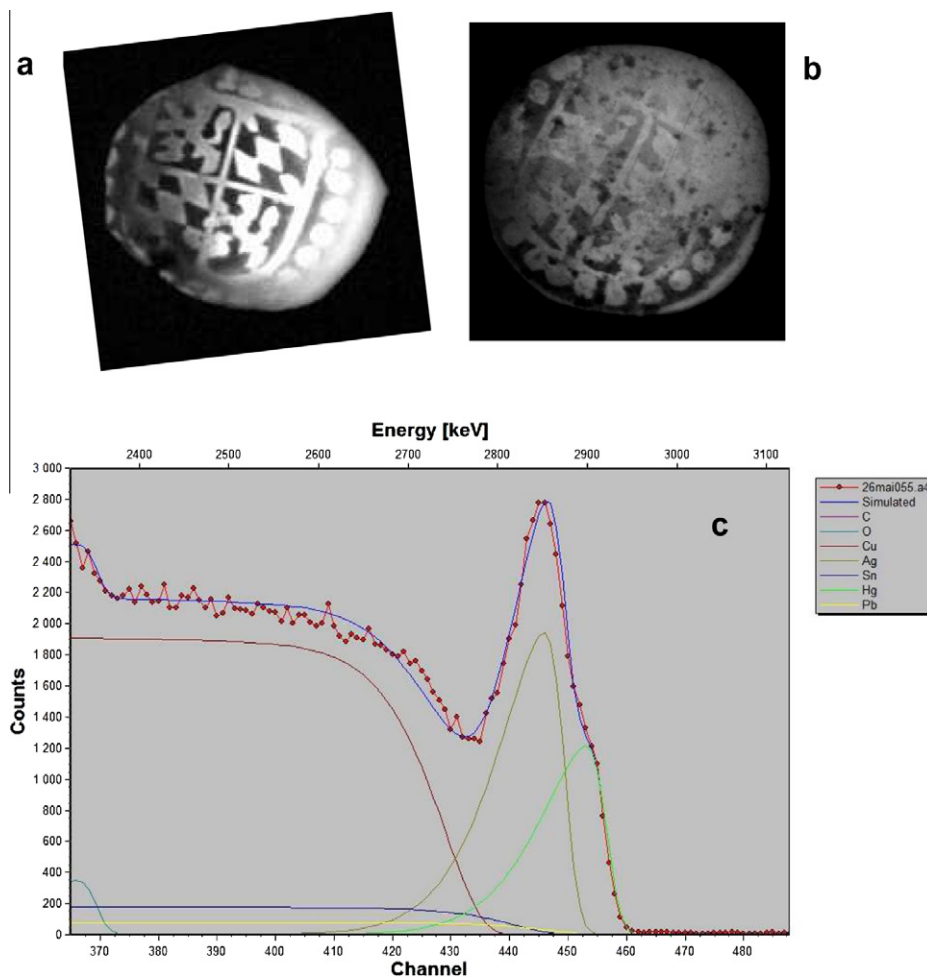


Fig. 2. (a) Official coin of Johann August von der Pfalz-Veldenz (1598–1611); (b) imitation of (a); (c) 3 MeV proton RBS spectrum of coin (b).

range has been confirmed by archaeometallurgical replication studies [21].

The silvering technology applied in the case of the counterfeit coins struck with the arms of the city of St Gallen and Chur (Swiss Confederation) does not use mercury. The silver coating is less well preserved and the corrosion layer too thick for RBS studies. A small fragment was observed under microscope showing a thin layer of pure silver (Fig. 3), but this observation was not sufficient to determine the plating method. Replications have demonstrated that either application of a thin silver foil or chemical reaction (chemical replacement of copper of the substrate by silver in solution) produce such a very thin and pure layer of silver.

2.2.2. The altered and restored surface

The corrosion of the silver–copper alloys and the effect of their surface cleaning procedures have already been studied by the combination of PIXE with RBS [22]. In this contribution, we are dealing with another aspect of restoration concerning the application of protective varnishes on the fragile objects, in particular wood and archaeological bones. This procedure is wide-spread and can influence the results of the element analysis by PIXE. For example, the analysis of a varnished part and an original part of the same prehistoric object gives different compositions due to the attenuation of the X-rays through the varnish layer (Table 1). The carbon signal, corresponding to the varnish layer of approx. 3–4 μm thickness, can be clearly observed on the RBS spectrum (Fig. 4). The composition and the thickness of the varnish could be taken into

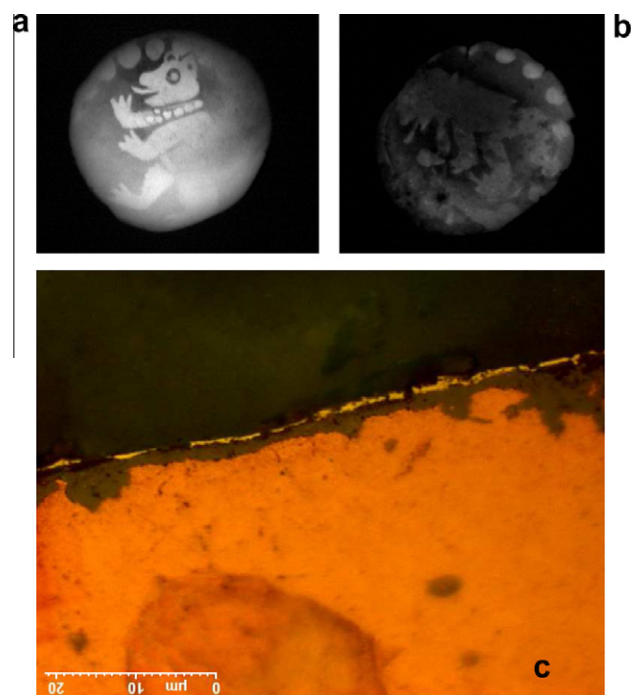


Fig. 3. (a) Official coin of St Gallen (Swiss Confederation); (b) imitation of (a); (c) metallographic observation of a fragment of (a).

account to correct the attenuation of the Na, Mg, P, Ca K-lines and obtain reliable composition. Accurate values for these elements are particularly important for the characterisation of the archaeological bones [23] and for distinguishing ancient ivory, bone and antler [24].

More generally, in the case of corroded/alttered as well as restored objects, the surface modification has to be taken into account for PIXE analyses. RBS provides a necessary complement for this “quality control”.

Table 1
PIXE analysis with 3 MeV protons of an ancient bone (scapula of herbivore) discovered in the Pataud shelter in Dordogne (30 000 BP).

Concentration (wt.%)	Ancient bone (30 000 BP)		Comparison with estimated values for modern bone, from [23,29]
	Varnished sample mean (min–max)	Virgin sample	
Na ₂ O	0.26 (0.15–0.4)	0.55	1
MgO	0.36 (0.3–0.4)	0.55	1
P ₂ O ₅	26.2 (25–29)	35.6	42
CaO	63.1 (60–65)	58.6	56

2.2.3. Light element quantification

As shown below, backscattering spectrometry (BS) using 3 MeV protons is very sensitive to light elements. These conditions are well adapted to the quantification of C and O for which the non-Rutherford cross-sections are multiplied by 13 and 7, respectively. In a previous publication [12] it has been demonstrated that quantitative analysis, including C and O, was achieved for the characterisation of paint by using 3 MeV protons for simultaneous PIXE and BS. The proportion of binder to pigment was, for the first time, determined in paintings of the Italian Renaissance [13].

Looking for carbon in prehistoric paintings or bones is also very important for radiocarbon dating. It is the only way to obtain absolute dates for prehistoric art [25]. So, we recently developed PIXE and RBS mappings for detecting carbon in painting samples collected in Tassili-n-Ajjer in Algeria [15]. The same procedure was applied on a modern bone in order to measure the organic phase mainly composed of collagen. The carbon signal is clearly shown on the RBS spectrum (Fig. 5a) illustrating a good preservation of the organic components. By comparison with the previous examples presented in Section 2.2.2, we can see that we are able to discriminate three different cases: a modern bone with well preserved collagen, an ancient bone where the collagen has completely disappeared due to the ageing process, and an ancient bone without collagen remains but covered with a modern varnish. Furthermore, PIXE and RBS mappings can detail the distribution of the

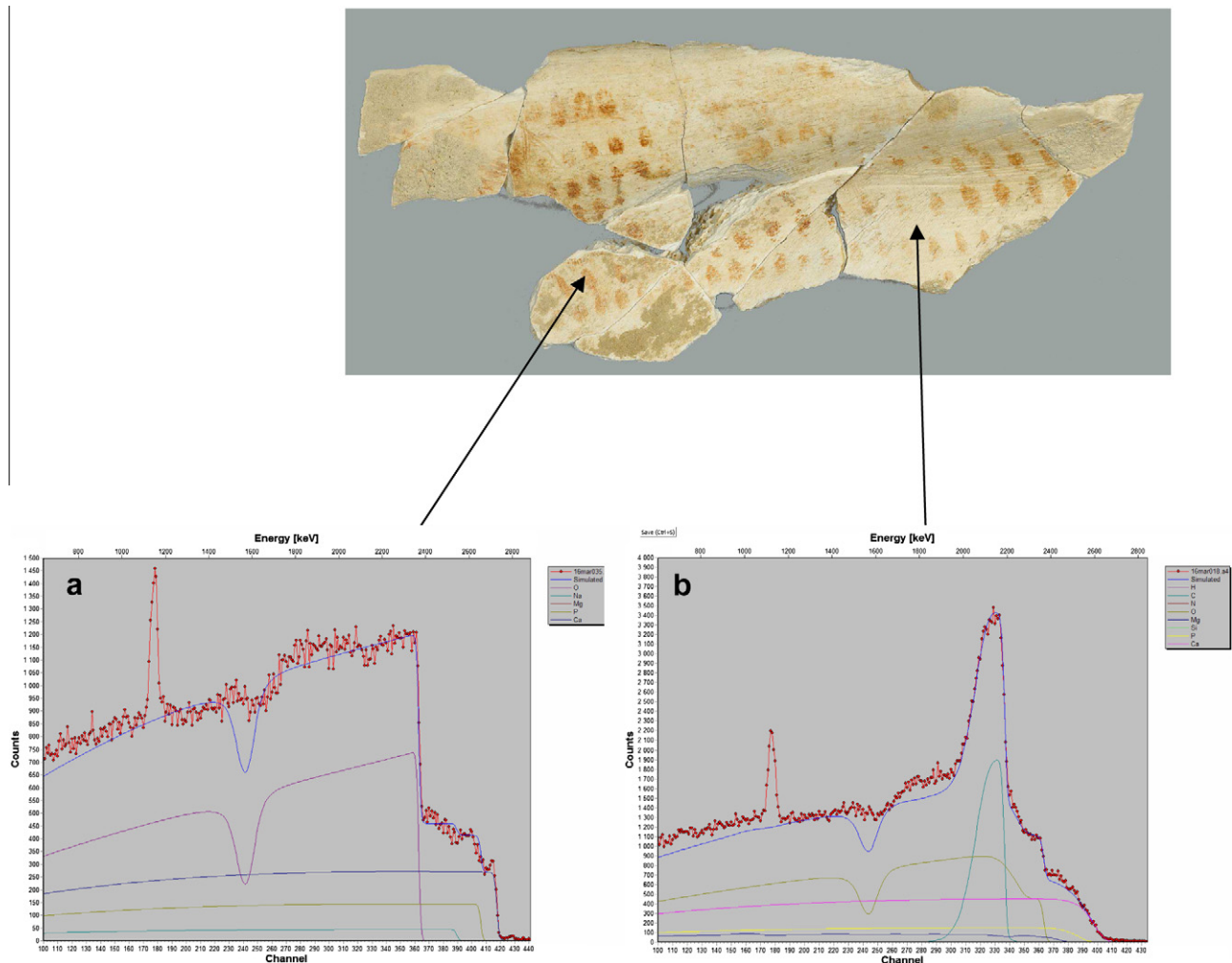


Fig. 4. Backscattered 3 MeV proton spectra of an ancient bone (scapula of herbivore) discovered in the Pataud shelter in Dordogne (30 000 BP): (a) sample without restoration; (b) sample covered with varnish.

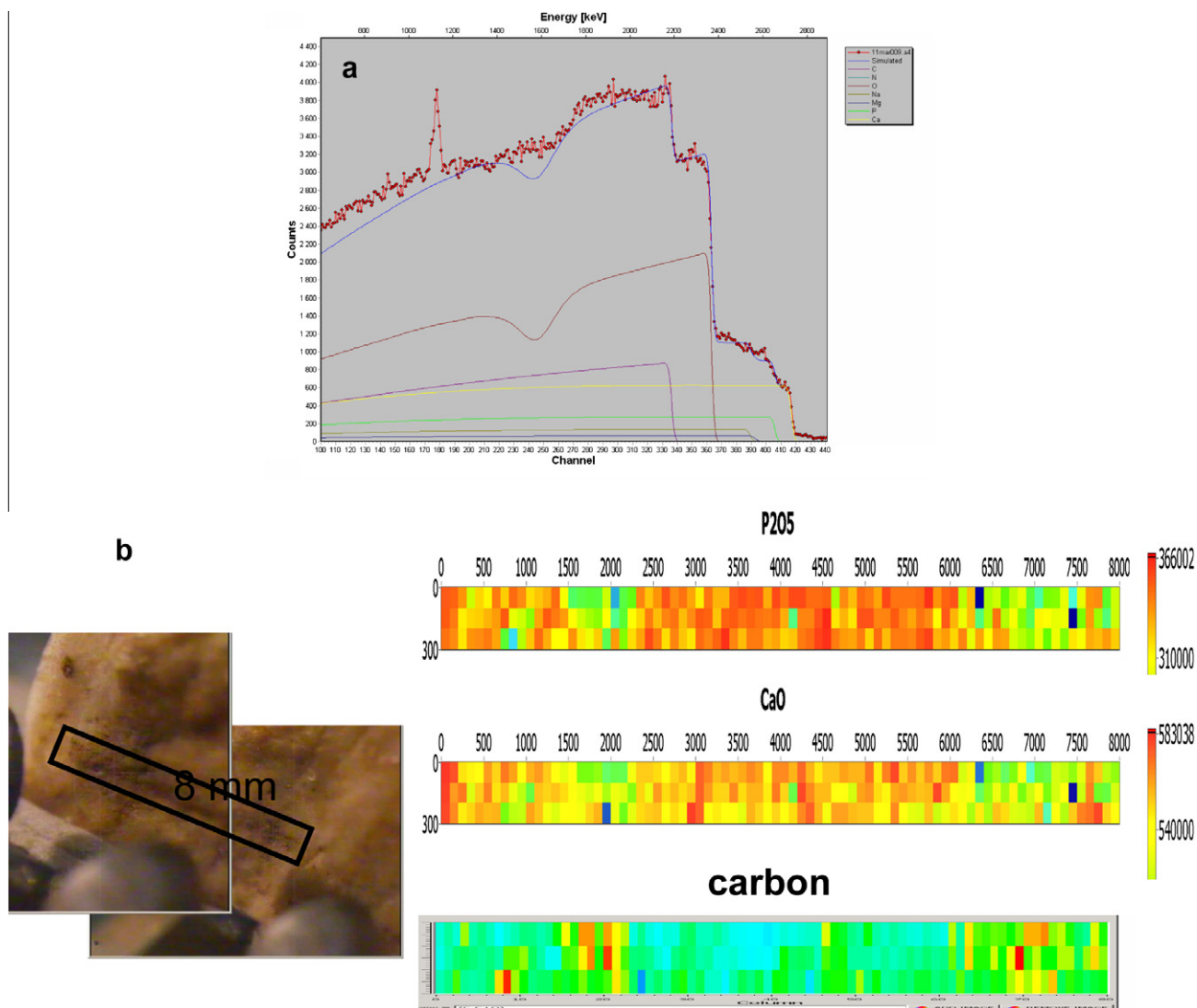


Fig. 5. (a) Backscattered 3 MeV proton RBS spectrum of a modern bone; (b) PIXE concentration maps in CaO, and P₂O₅ (in ppm) and RBS carbon distribution.

elements in bone (Fig. 5b). The heterogeneities observed in this case are mainly due to surface contamination.

By using 3 MeV protons as incident particles the limits of detection for carbon in bone can be estimated to 5 at.%. Better limits could be achieved by (d, p) nuclear reactions but deuterons are not always available. NRA experiments can also be used to check the biological origin of the carbon by detecting the nitrogen associated with carbon in collagen [26].

3. X-radiography using AGLAE

The conventional radiography shows low sensitivity to chemical nature when the elements have close electron densities [27]. However, when using monochromatic X-rays, it is possible to enhance the absorption of a particular element and to reveal chemical contrasts. Although this is a powerful application of the synchrotron radiation [28], we have tested the possibility of doing X-radiography using monochromatic X-rays produced by bombarding a metal target with charged particles.

For this purpose, the milli-beamline of AGLAE was used for producing 3 MeV proton beam with current of approx. 1 μ A. A metal target, selected taking into account the object to be X-rayed, is

bombarded by the particles and characteristic K and L lines are emitted (Fig. 6). The irradiated area is about 15 cm by 15 cm.

A first case of application was a painting by the Flemish school (1575–1599). The base pigment for this period was lead white,

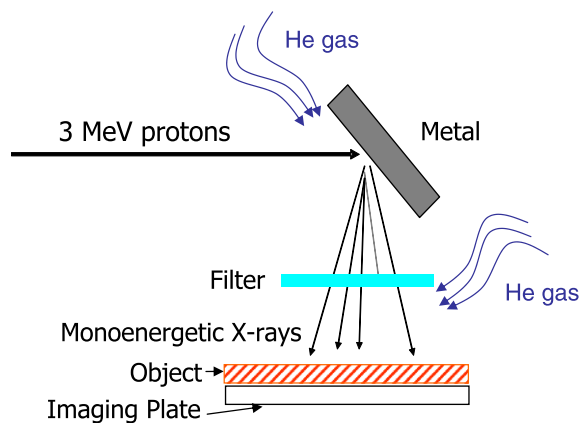


Fig. 6. Principle of the production of monochromatic X-rays by using 3 MeV protons.

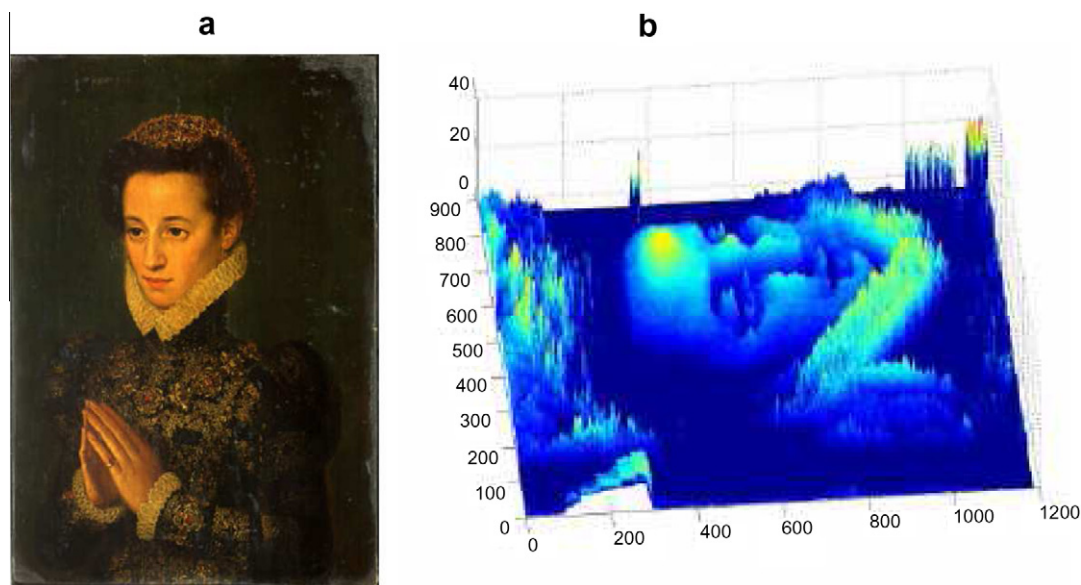


Fig. 7. (a) Painting of the Flemish school (1575–1599), 'Dame en prière', Louvre museum; (b) thickness of lead white calculated from monochromatic radiography.

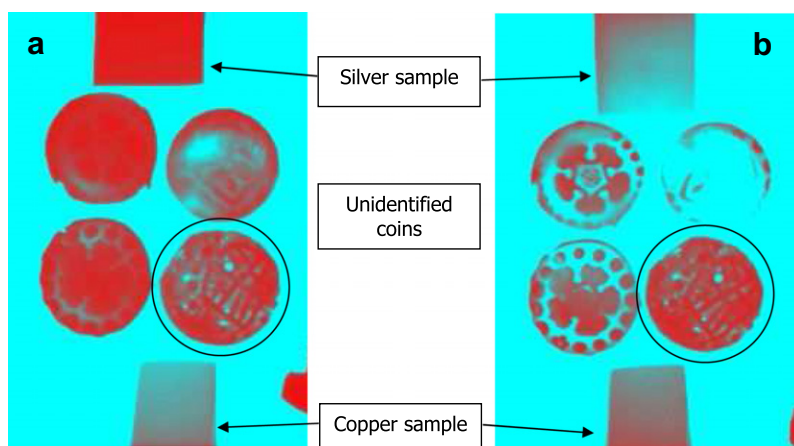


Fig. 8. X-radiographs of billon (poor silver–copper alloy) and copper coins covered by a thick corrosion layer: (a) with Sn $K\alpha$ line at 25.3 keV; (b) with Sb $K\alpha$ line at 26.4 keV. Only the copper coin indicated by a circle and the copper sample are not sensitive to the X-ray energy variation.

which was mainly used to paint flesh tones or light tint. Different metals have been tested as secondary targets. The best contrast was obtained by using Zr or Sn. L lines were attenuated by an aluminium or a titanium filter. The intensity of the X-radiographic image was then converted into lead white thickness using the Beer–Lambert attenuation law calibrated with known thicknesses of pigment (Fig. 7). Lead white layers from a few to 30 μm thick were calculated. The variation of the incident of X-rays angles through the painting layer was neglected for the calculation.

The second case concerned ancient coins made of silver–copper alloy. Due to the corrosion layer, it is not possible to distinguish billon (poor silver–copper alloy) coins from copper ones. Two metal targets were selected for contrast imaging. Sn emits a $K\alpha$ line at 25.3 keV corresponding to the pre-edge region of the Ag–K absorption threshold and Sb at 26.4 keV corresponding to the post-edge region of the Ag–K absorption threshold. Even if the X-rays are not purely monochromatic (mainly due to the $K\beta$ emission) it is possible to isolate the coin made of pure copper (without silver) by observing similarities between both X-photographs (Fig. 8). On the contrary, coins containing silver present a marked contrast due to the abrupt change of absorption on both sides of the Ag–K

edge. The remaining dark areas, representing a flower on the silver coins, are due to thicker areas, and not to copper products.

X-radiography using chemical contrast enables pure copper and silver–copper alloy to be discriminated and identification to be done without any cleaning intervention to the coins.

4. Conclusion

This contribution concentrates on the recent developments of the application of the external ion beam to the characterisation of various materials of the cultural heritage. It is demonstrated how the combination of PIXE and RBS provides useful information on the manufacturing of lustre-decorated ceramics and on the silvering technology. The collection of such a large number of data would have never been possible without the contribution of these non-destructive techniques. In addition, RBS plays an important part in PIXE analysis by giving access to the light element quantification in biomaterials or in mixed compounds and, by controlling the depth uniformity. These last aspects are very important in the archaeological and museum fields because of the deterioration and

successive restorations of the objects. Finally, we have presented preliminary results concerning monochromatic X-radiography induced by protons. This technique seems to be promising for chemical contrast applications.

Acknowledgement

This manuscript is the direct continuation of the work of our regretted colleague Joseph Salomon who passed away 2 years ago. The merit of this article is largely his.

The authors would like to thank E. Alloin from the PAIR Center, Sélestat, France for her collaboration on the Preuschoorf hoard and L. Chiotti and R. Nespoulet from the Muséum National d'Histoire Naturelle, France for providing the archaeological scapula from Abri Pataud.

References

- [1] H.-E. Mahnke, A. Denker, J. Salomon, C. R. Phys. 10 (2009) 660.
- [2] T. Calligaro, A. Mossmann, J.-P. Poirrot, G. Querré, Nucl. Instr. Meth. 136–138 (1998) 846.
- [3] L. Bellot-Gurlet, G. Poupeau, J. Salomon, Th. Calligaro, B. Moignard, J.-C. Dran, J.-A. Barrat, L. Pichon, Nucl. Instr. Meth. 240 (2005) 583.
- [4] L. Beck, M. Lebon, L. Pichon, M. Menu, L. Chiotti, R. Nespoulet, P. Paillet, X-ray Spectrometry 40 (2011) 219–223.
- [5] P.A. Mandò, M.E. Fedi, N. Grassi, A. Migliori, Nucl. Instr. Meth. 239 (2005) 71.
- [6] M.F. Guerra, Nucl. Instr. Meth. 226 (2004) 185.
- [7] Ž. Šmit, J. Istenič, T. Knific, Nucl. Instr. Meth. 266 (2008) 2329.
- [8] G. Demortier, J.-L. Ruvalcaba-Sil, Nucl. Instr. Meth. 239 (2005) 1.
- [9] S. Röhrs, T. Calligaro, F. Mathis, I. Ortega-Feliu, J. Salomon, P. Walter, Nucl. Instr. Meth. 249 (2006) 604.
- [10] J. Salomon, J.-C. Dran, T. Guillou, B. Moignard, L. Pichon, P. Walter, F. Mathis, Nucl. Instr. Meth. B 266 (2008) 2273.
- [11] F. Mathis, B. Moignard, L. Pichon, O. Dubreuil, J. Salomon, Nucl. Instr. Meth. 240 (2005) 532.
- [12] L. Beck, L. de Viguier, Ph. Walter, L. Pichon, P.C. Gutiérrez, J. Salomon, M. Menu, S. Sorieul, Nucl. Instr. Meth. B 268 (2010) 2086.
- [13] L. de Viguier, L. Beck, J. Salomon, L. Pichon, Ph. Walter, Anal. Chem. 81 (2009) 7960.
- [14] J. Salomon, J.-C. Dran, T. Guillou, B. Moignard, L. Pichon, Appl. Phys. A 92 (2008) 43.
- [15] L. Pichon, L. Beck, Ph. Walter, B. Moignard, T. Guillou, Nucl. Instr. Meth. B 268 (2010) 2028.
- [16] A. Polvorinos del Rio, J. Castaing, M. Aucouturier, Nucl. Instr. Meth. B 249 (2006) 596.
- [17] D. Chabanne, A. Bouquillon, M. Aucouturier, X. Dectot, G. Padeletti, Appl. Phys. A 92 (2008) 11.
- [18] G. Padeletti, G. Ingo, A. Bouquillon, S. Pages Camagna, M. Aucouturier, S. Roehrs, P. Fermo, Appl. Phys. A 83 (2006) 475.
- [19] W.A. Oddy, Endeavour 15 (1991) 29.
- [20] L. Beck, E. Alloin, U. Klein, T. Borel, C. Berthier, A. Michelin, Revue de Numismatique 166 (2010) 199–218.
- [21] A. Michelin, L. Beck, E. Alloin, D. Robcis, F. Téreygeol, in: F. Téreygeol (Ed.), Paléométallurgies et Expérimentations, Recherches sur les Chaînes de Production des Métaux aux Périodes Anciennes, Projet Collectif de Recherche, SRA Poitou-Charentes, 2008, p. 122.
- [22] L. Beck, E. Alloin, C. Berthier, S. Réveillon, V. Costa, Nucl. Instr. Meth. B 266 (2008) 2320.
- [23] I. Reiche, L. Favre-Quattropani, Th. Calligaro, J. Salomon, H. Bocherens, L. Charlet, M. Menu, Nucl. Instr. Meth. B 150 (1999) 656.
- [24] K. Müller, C. Chadeaux, J. Rodière, L. Chiotti, R. Nespoulet, C. Vercoutère, M. Menu, I. Reiche, Metalla Sonderheft 2 (2009) 78.
- [25] H. Valladas, Meas. Sci. Technol. 14 (2003) 1487.
- [26] N. Boscher-Barre, P. Trocellier, Nucl. Instr. Meth. B 73 (1993) 413.
- [27] D. Creagha, Physical Techniques in the Study of Art, Archaeology and Cultural Heritage, vol. 2, 2007, p. 1.
- [28] L. Bertrand, Physical Techniques in the Study of Art, Archaeology and Cultural Heritage, vol. 2, 2007, p. 97.
- [29] Y.X. Zhang, Y.S. Wang, Y.P. Zhang, G.L. Zhang, Y.Y. Huang, W. He, Nucl. Instr. Meth. B 260 (2007) 178.